

Direct measurements of quantum kinetic energy tensor in stable and metastable water near the triple point: an experimental benchmark

Carla Andreani,[†] Giovanni Romanelli,[¶] and Roberto Senesi^{*,†}

Università degli Studi di Roma "Tor Vergata", Dipartimento di Fisica e Centro NAST, Via della Ricerca Scientifica 1, 00133 Roma, I, Consiglio Nazionale delle Ricerche, CNR-IPCF, Sezione di Messina, I, and ISIS Neutron Source, Science Technology Facility Council, Chilton, Oxfordshire, OX11 0QX, UK

E-mail: roberto.senesi@uniroma2.it

*To whom correspondence should be addressed

[†]Università degli Studi di Roma "Tor Vergata", Dipartimento di Fisica e Centro NAST, Via della Ricerca Scientifica 1, 00133 Roma, I

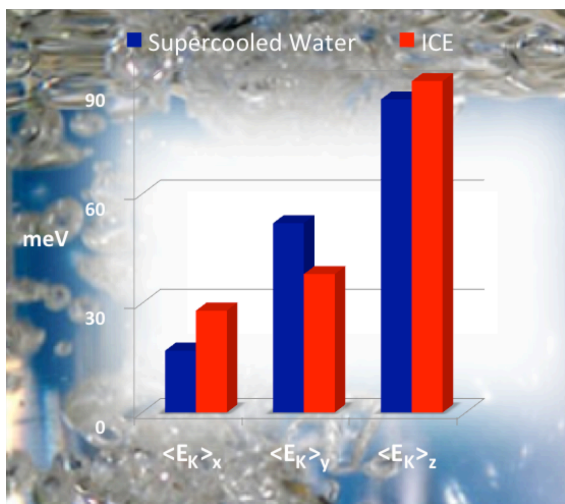
[‡]Consiglio Nazionale delle Ricerche, CNR-IPCF, Sezione di Messina, I

[¶]ISIS Neutron Source, Science Technology Facility Council, Chilton, Oxfordshire, OX11 0QX, UK

Abstract

This study presents the first direct and quantitative measurements of the nuclear momentum distribution anisotropy and the quantum kinetic energy tensor in stable and metastable (supercooled) water near its triple point using Deep Inelastic Neutron Scattering (DINS). From the experimental spectra accurate lineshapes of the hydrogen momentum distributions are derived using an anisotropic Gaussian and a model independent framework. The experimental results, benchmarked with those obtained for the solid phase, provide the state of the art directional values of the hydrogen mean kinetic energy in metastable water. The determinations of the direction kinetic energies in the supercooled phase, benchmarked with ice at the same temperature, provide accurate and quantitative measurements of these dynamical observables in metastable and stable phases, i.e. key insight in the physical mechanisms of the hydrogen quantum state in both disordered and polycrystalline systems. The remarkable findings of this study establish novel insight to further expand the capacity and accuracy of DINS investigations of the nuclear quantum effects in water and represent reference experimental values for theoretical investigations.

TOC Graphic:



keywords: deep inelastic neutron scattering; ab initio path integral molecular dynamics; particle momentum distribution

A large number of experimental and theoretical dynamical studies of liquid water near the triple point are available in literature¹⁻⁹ nevertheless an full and accurate characterization of hydrogen dynamics is still lacking. The latter is of vital importance for clarifying thermodynamic properties

and the key to expand our understanding of some of the mysterious characteristics of water, supercooled water (SW) and glassy water, the latter being its viscous counterparts, known as amorphous ice.¹⁰

Nuclear Quantum Effects (NQE) play an important role in water, ice and hydrogen-bonded systems and directly influence their microscopic structure and dynamical properties. In most of these cases, the hydrogen atoms are localized in potential well with pronounced zero point motion. The equilibrium hydrogen dynamics is reflected in the quantum momentum distribution, $n(p)$, a quantity which provides complementary information to what is garnered from diffraction techniques. Due to NQEs $n(p)$ markedly differs from the classical Maxwell-Boltzmann distribution, and is determined almost entirely by the quantum mechanics of the vibrational ground state properties.^{11–17} This makes $n(p)$ a highly sensitive probe of the local environment, fingerprinting any changes occurring both in the structure of the hydrogen-bonded network as well as in the local symmetry. Thus $n(p)$ together with the mean kinetic energy, $\langle E_K \rangle$, provide unique key insights into the hydrogen local environment to rationalize the puzzling feature of liquid water near the triple point. DINS is the unique experimental technique that directly access the $n(p)$.¹⁸ The basic principles of data interpretation of the DINS technique are based on the validity of the Impulse Approximation (IA)¹⁹ which is exact in the limit of infinite momentum transfer, $\hbar q$.^{20,21} Within the IA, the inelastic neutron scattering cross-section directly probes the $n(p)$ of each nucleus in the target system.¹¹ Many DINS experiments have uncovered the hydrogen $n(p)$ in a large variety of water systems showing how its line shape fingerprints the change in the hydrogen network. Recent examples are DINS in water and ice reflecting the breaking and distortion of the hydrogen bonds that occurs upon melting²² or the competition between intra and inter molecular NQEs unraveled by measuring the anisotropy of the quantum kinetic energy tensor of D and O in D₂O.^{10,23} Recent Inelastic Neutron Scattering (INS) studies of ice, water, SW and amorphous ices (Low Density, High Density and Very High Density) measurements show that, in an harmonic framework, almost identical value of $\langle E_K \rangle_z$, the OH stretching component of the $\langle E_K \rangle$, are obtained: 98 meV, 100 meV, 100 meV and 99-101 meV, respectively.^{10,24} This is an indication that the NQEs on the OH stretching frequency, ω_z , is weakly dependent in the temperature range explored. On the contrary DINS measurements go beyond the harmonic framework and provide full directional components of the mean kinetic energy tensor.¹⁰

From the theoretical point of view empirical flexible and polarizable models^{2,5} are not able to fully capture the small difference between the $n(p)$ distributions of water near its triple point one observes in DINS and INS experiment. First principles molecular dynamics such as open Path Integral Car-Parrinello Molecular Dynamics (PICPMD), unlike less transferable models, is a promising path for the exploration of these detailed features in $n(p)$ and $\langle E_K \rangle$.³ In particular in a DINS experiment on ice the quantum $\langle E_K \rangle$ has been measured on ice at 271 K, and the observable has been used as a quantitative benchmark for electronic density functionals employed using a PICPMD in the description of hydrogen bonded systems in *ab initio* numerical simulations.²⁵ Beyond ice, path integral simulation studies are employed to study diluted water phase such as supercritical water.⁴ In these cases experimental and theoretical predictions of $\langle E_K \rangle$ are in satisfactory quantitative agreement. On the other hand discrepancies still exists between experiments and theory for liquid water at room temperatures and below. Particularly significant is the excess of $\langle E_K \rangle$ across the density maximum at 277 K and across the supercooled phase at 272 K observed in DINS experiments.^{26–28} Similar excess of $\langle E_K \rangle$ is also found in supercooled heavy water⁷ and highly pressurized SW.⁸ The interpretation of these experiments is still matter of debate. Indeed

in the case of SW at $T=271$ K an excess of $\langle E_K \rangle$, about 58% (8 kJ/mol) higher with respect to the room-temperature result,^{26–28} seems to be incompatible with the experimental molecular structure of water. Yet the proposed explanations are not supported by any computer simulation calculation or theoretical model. Very recent path integral molecular dynamics provide accurate results for nuclear momentum distribution and²⁹ of water near the triple point. Thus accurate DINS experimental determination are advisable in order to allow an quantitative cross comparison between DINS experimental and simulation determinations of the $n(p)$.

In this paper we present a DINS study of water near the triple point to determine accurate measurements of hydrogen $n(p)$ and hydrogen directional mean kinetic energy components, $\langle E_K \rangle_\alpha$. The single particle dynamics in SW and ice at $T=271$ K and water at 300 K, is investigated employing new experimental and cooling set up. The measurement on ice is specifically recorded at the same temperature used in Ref.²⁵ in order to allow a quantitative benchmark with measurement on SW. The DINS measurements are carried out on the VESUVIO beamline at the ISIS pulsed neutron and muon source (Rutherford Appleton Laboratory, Chilton, Didcot, UK).^{30–33} In the DINS experiment we obtain, from each l -th detector, a Neutron Compton Profile (NCP) for the hydrogen nuclei, $F_l(y, q)$. These functions represent the hydrogen longitudinal momentum distribution. Full details on DINS formalism, detailed description of operation of VESUVIO instrument, sample preparation and experimental set up, procedure of cooling and phase monitoring, measurements and data analysis are reported in the Supporting Information. The experimental angular average of the $F_l(y, q)$ functions, namely $\bar{F}(y, q)$, for SW at $T = 271$ K is plotted in the top panel of Figure 1, together with the angle averaged experimental resolution function, $\bar{R}(y, q)$ (for full detail see SM). Figures of similar statistical accuracy have been obtained for the other DINS data sets of ice and water samples.

Primary goal of this study is to derive the $n(p)$ lineshapes, $\langle E_K \rangle$ and its directional components, $\langle E_K \rangle_\alpha$, from the set of $F(y, q)$ spectra. For each sample a simultaneous fit of the individual $F_l(y, q)$ spectra is accomplished using two parametric models for the $n(p)$: (a) a model-independent lineshape, hereafter named Model 1 (M1) and (b) a three dimensional anisotropic Gaussian lineshape derived from a quasi harmonic model, hereafter named Model 2 (M2). The latter is recently employed to reveal the local environment of hydrogen in polycrystalline ice,^{22,25} amorphous ice¹⁰ and heavy water.²³ Then experimental $n(p)$ in M1 is given by the Gauss-Laguerre expansion^{12,20,26}

$$n_{M1}(p) = \frac{\exp\left(-\frac{p^2}{2\sigma^2}\right)}{(\sqrt{2\pi}\sigma)^3} \sum_n c_n (-1)^n L_n^{\frac{1}{2}}\left(\frac{p^2}{2\sigma^2}\right), \quad (1)$$

where $L_n^{\frac{1}{2}}$ are the generalized Laguerre polynomials, and c_n the expansion coefficients from which, together with the standard deviation, σ , one can derive the momentum distribution lineshape.

The experimental $n(p)$ lineshapes in M2 is determined by modeling the momentum distributions as spherical averages of multivariate Gaussians according to²⁵

$$4\pi p^2 n_{M2}(p) = \left\langle \frac{\delta(p - |\mathbf{p}|)}{\sqrt{8\pi^3 \sigma_x \sigma_y \sigma_z}} \exp\left(-\frac{p_x^2}{2\sigma_x^2} - \frac{p_y^2}{2\sigma_y^2} - \frac{p_z^2}{2\sigma_z^2}\right) \right\rangle \quad (2)$$

where σ_z is along the direction of the H bond, and σ_x and σ_y are in the plane perpendicular to the direction of the H bond, *i.e.*. The set of parameters, $\sigma_{x,y,z}$, determine the anisotropy in the momentum

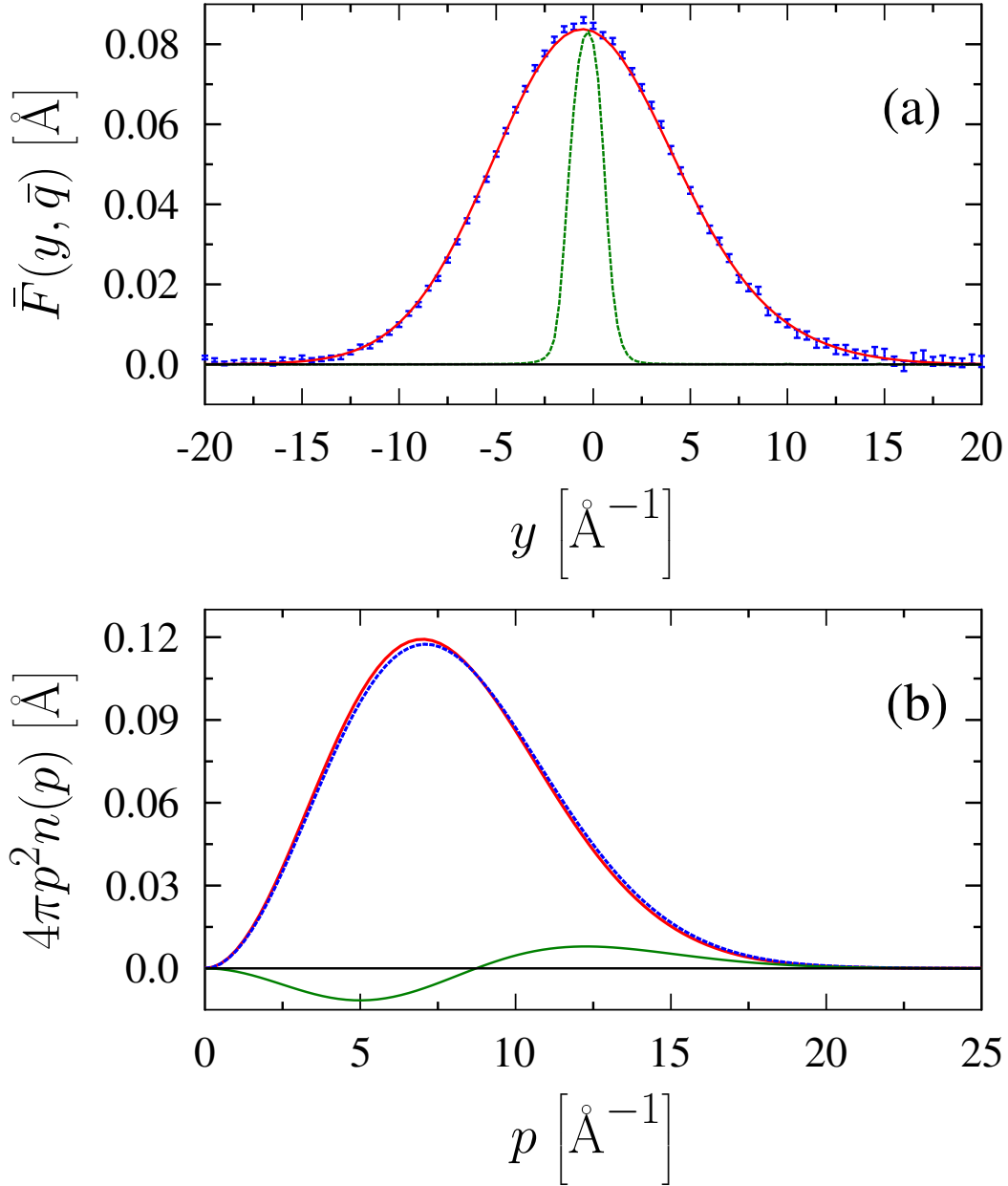


Figure 1: (colour online) (a) Angle averaged hydrogen NCP $\bar{F}(y, q)$ for SW at $T = 271$ K **blue error bars**. The best fit of this function using M2 is plotted as **red line**. The experimental resolution $R(y, q)$ is plotted as **green line**. (b) Radial momentum distributions $4\pi p^2 n(p)$ for SW (**blue line**) and ice (**red line**) at $T = 271$ K. The difference between SW and ice line-shapes (magnified by a factor of 10) is plotted as a **green line**.

Table 1: (colour online) The $\langle E_K \rangle$ and individual $\langle E_K \rangle_\alpha$ values, from present DINS measurements in bulk SW and ice at $T = 271$ K are shown. These are obtained using M2, while $\langle E_K \rangle$, c_4 and σ values using M1. The latter is found to be equal to $\bar{\sigma} = \sqrt{\sum \sigma_\alpha^2/3}$ where the σ_α are from M2.

T	[K]	SW 271	Ice 271	Ice ²⁵ 271
M1				
σ	[Å ⁻¹]	5.01±0.02	5.03±0.03	5.01±0.03
c_4		0.11±0.01	0.11±0.02	0.10±0.01
$\langle E_K \rangle$	[meV]	156.0±2.0	157.0±2.0	156.0±2.0
M2				
σ_x	[Å ⁻¹]	2.9±0.5	3.7±0.1	3.7±0.3
σ_y	[Å ⁻¹]	5.0±0.5	4.3±0.3	4.3±0.4
σ_z	[Å ⁻¹]	6.5±0.2	6.6±0.2	6.5±0.4
$\langle E_K \rangle_x$	[meV]	17±5	28±2	29±4
$\langle E_K \rangle_y$	[meV]	52±10	38±5	38±9
$\langle E_K \rangle_z$	[meV]	86±5	91±5	87±9
$\langle E_K \rangle$	[meV]	156.0±2.0	157.0±2.0	154.0±2.0

distribution lineshape. We recall that although the M1 model represents the most general momentum distribution lineshape, it does not allow to directly separate the effects of anharmonicity from those of anisotropy.^{1,11,25}

Top part of Figure 1 shows the $\bar{F}(y, q)$ function for SW at $T=271$ K, and its best fit, resulting from model M2. The quality of present data is quite good and the accuracy comparable to previous benchmark experiment on polycrystalline ice:²⁵ the difference between the experimental data and the best fit is within two error bars. This is obtained by the difference between data and fits, both normalized to unity area. The deviations from Gaussian momentum distribution found in SW and ice using model M1 (see the non-zero c_4 coefficients in Table 1) can be entirely ascribed to the anisotropy of the momentum distribution. The σ_α values reported in Table 1 unveil a main distinctive feature between SW and ice at $T = 271$ K: the anisotropy of the momentum distribution is slightly more pronounced in SW than in the solid phase. Similar features are also obtained in previous combined INS and DINS investigation in water at $T=285$ K and ice at $T=271$ K.²² The difference in the two $n(p)$ lineshapes, magnified by a factor ten, is untangled in the bottom panel of Figure 1. This shows the radial momentum distributions, $4\pi p^2 n(p)$, for SW and ice obtained using the M2 model. The high momentum components in $n(p)$ are highly sensitive to, and dominated by, the curvature of the effective hydrogen potential. The anisotropic character of the $n(p)$ is due to the anisotropy of the potential that the hydrogens experience along different molecular directions.²⁻⁵

Values of the hydrogen total mean kinetic energy, $\langle E_K \rangle = 3\frac{\hbar^2 \sigma^2}{2m}$, and the directional components along the three axes, $\langle E_K \rangle_\alpha = \frac{\hbar^2 \sigma_\alpha^2}{2m}$, are reported in Table 1. Table 2 compares our $\langle E_K \rangle$ values for ice, SW and liquid water with values obtained from INS²⁴ and theory.⁹ The $\langle E_K \rangle$ value for ice at $T=271$ K derived in this experiment from M1 together with the σ_α values are the same, within the experimental uncertainties, with those obtained in previous measurement at the same

temperature.²⁵ This is a reference benchmark which validates and strengthens the total value of $\langle E_K \rangle = 156$ meV, and its directional σ_α components obtained for SW.

Several are the experimental investigations showing red-shift in the OH stretching occurring from liquid to solid (see Table 2 and Figure 2), interpreted as a fingerprint of stronger H-bonding in ice respect to water.^{35,36} Changes in the directional components of the $\langle E_K \rangle_\alpha$ are used to monitor the competing NQEs associated to phase changes in water near its triple point.²³ These reflect the entanglement of the potential energy surface with $n(p)$ that is generated by the uncertainty relation between position and momentum of the hydrogen atom: this is the result of a competition between anharmonic quantum fluctuations of intermolecular bond bending and intramolecular covalent bond stretching. The latter fluctuations strengthens H-bonds whereas the former weakens H-bonds.²² Thus in the case of SW and ice the competition between the directional energy components $\langle E_K \rangle_\alpha$ is such to produce a subtle cancellation effect, resulting in $\langle E_K \rangle$ values close to each other. The DINS technique effectively fingerprints the competition between intra and inter molecular NQEs during the transition from disordered phase (SW) to polycrystalline one (ice). Further result of the present investigation is that $\langle E_K \rangle$ value in SW is slightly lower than in ice at the same temperature, in quantitative agreement with Ref.²⁹ and qualitative agreement with Ref.⁶

As far as the comparison between metastable liquid (SW) and water at room temperature is concerned we find the following results: $\langle E_K \rangle$ in SW is about 7% and 9% in excess respectively to $\langle E_K \rangle$ values in the stable liquid at $T=300$ K, which are $\langle E_K \rangle = 146$ meV from the present study, and $\langle E_K \rangle = 143$ meV from Ref.⁴ (see Table 2 and Figure 2).

From Table 2 the experimental result for SW and ice at $T = 271$ K are in quite good agreement with INS data;²⁴ in the case of ice a good comparison is also seen with predictions from an harmonic theoretical model.⁹ Although the harmonic model is successful in reproducing $\langle E_K \rangle$ of ice at $T = 271$ K it overestimates the value of $\langle E_K \rangle$ at ambient temperature. This occurs because harmonic models cannot fully account for the softening of the ground state potential energy surface at room temperature in water, in agreement with previous suggestion from a joint DINS and path integral investigation.⁴ Results from a path integral molecular dynamics simulation⁶ on SW and ice at $T=270$ K are instead both approximately 8 meV lower than the present experimental results.

In this study we derive new quantitative and accurate values for the hydrogen $n(p)$, $\langle E_K \rangle$ and directional $\langle E_K \rangle_\alpha$ observables in water near the triple point. To the best of our knowledge the present value of $\langle E_K \rangle = 156$ meV at 271 K in SW represents the most reliable experimental value obtained so far, since it is established through a benchmark measurement on ice at $T=271$ K, which is correlated with previous DINS result on ice at the same temperature.²⁵ The $\langle E_K \rangle$ value in SW is found approximately 10 meV higher with respect to $\langle E_K \rangle$ value for water at room temperature, corresponding to less than 7% increase. Results from SW and ice at $T = 271$ K both show $n(p)$ functions with an anisotropic Gaussian lineshapes and directional anisotropic components of the $\langle E_K \rangle_\alpha$ tensor. The $\langle E_K \rangle$ value in SW can be regarded as an upper limit, which can help to identify those theories that best describe and explain the behaviour of water and hydrogen bonded systems.

The present DINS study provides a reference set of values of increased accuracy with respect to earlier measurements, yielding new and key insights in the three dimensional potential energy surface experienced by hydrogen in water near the triple point. DINS confirms to be a a unique and sophisticated technique for the investigation the NQEs in water. It is highly desirable to continue to expand the DINS accuracy in order to further refine the cross comparison with the parallel increasing accuracy of path integral molecular dynamics.

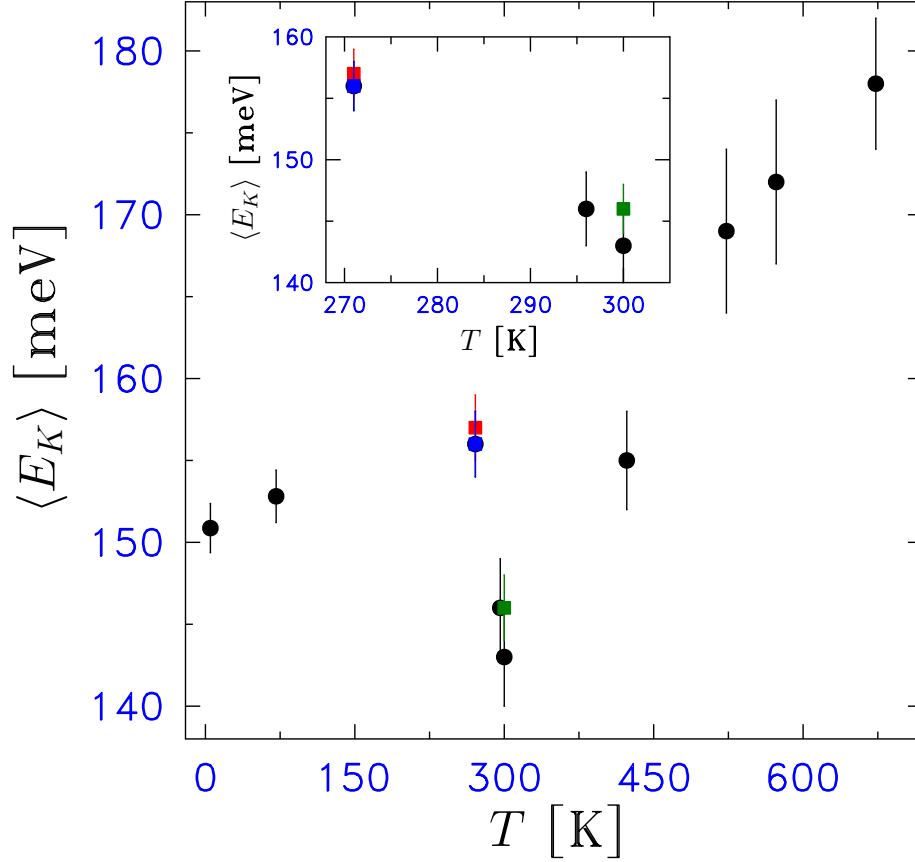


Figure 2: (colour online) (colour online) (a) $\langle E_K \rangle$ values for SW at $T=271$ K (blue full square), ice at $T=271$ K (red full square), and water at 300 K (green full circle) from present DINS study; (b) $\langle E_K \rangle$ values for ice at $T=5$ K, $T=71$ K³⁴ and $T=271$ K (black full square)²⁵ and water at 300 K and above (black full square) from previous DINS measurements.⁴ The insert shows a magnified picture in the temperature range 270 K - 305 K.

Table 2: (colour online) Values of $\langle E_K \rangle$ for SW, ice, and water. a) $\langle E_K \rangle^{DINS}$ values for SW from present study at T=271 K (blue), from path integral molecular dynamics simulation at T=270 K⁶ and from previous DINS experiments at T=269 K,²⁶ T=271 K²⁶ and T= 273 K;²⁷ $\langle E_K \rangle^{INS}$ values from previous INS experiment at the same corresponding temperatures;²⁴ b) $\langle E_K \rangle^{DINS}$ for ice from present study at T=271 K (red), from path integral molecular dynamics simulation at T=270 K⁶ and from previous DINS experiments at T=271 K;²⁵ $\langle E_K \rangle^{INS}$ value from previous INS experiment at T=271 K and $\langle E_K \rangle^M$ value from an harmonic theoretical model at T=271 K;⁹ c) $\langle E_K \rangle^{DINS}$ for water from present study at T=300 K(green) and from previous DINS experiments at T=300 K,⁴ $\langle E_K \rangle^{INS}$ and $\langle E_K \rangle^M$ values for water from previous studies.^{4,9,24,27}

Phase	T [K]	$\langle E_K \rangle^{DINS}$ [meV]	$\langle E_K \rangle^{INS}$ [meV]	$\langle E_K \rangle^M$ [meV]
SW	269	$(199 \pm 2)^{26}$	$(152 \pm 4)^{24}$	
	270			$(148.1 \pm 0.5)^6$
	271	156.0 ± 2.0 $(228 \pm 2)^{26}$	$(152 \pm 4)^{24}$	
	273	$(150 \pm 2)^{27}$	$(153 \pm 4)^{24}$	
Ice	270			$(149.5 \pm 0.5)^6$
	271	157.0 ± 2.0 $(156 \pm 2)^{25}$	$(158 \pm 4)^{24}$	$(155 \pm 3)^9$
Liquid	296	$(146 \pm 3)^{27}$	$(150 \pm 4)^{24}$	
	300	(146 ± 3) $(143 \pm 3)^4$		$(155 \pm 3)^9$

Acknowledgement

This work was supported within the CNR-STFC Agreement (2014-2020) concerning collaboration in scientific research at the ISIS pulsed neutron and muon source.

References

- (1) Reiter, G. F.; Li, J. C.; Mayers, J.; Abdul-Redah, T.; Platzman, P. The Proton Momentum Distribution in Water and Ice. *Brazilian Journal of Physics* **2004**, *34*, 142–147
- (2) Burnham, C. J.; Reiter, G. F.; Mayers, J.; Abdul-Redah, T.; Reichert, H.; Dosch, H. On the origin of the redshift of the OH stretch in Ice Ih: evidence from the momentum distribution of the protons and the infrared spectral density. *Physical Chemistry Chemical Physics (Incorporating Faraday Transactions)* **2006**, *8*, 3966
- (3) Morrone, J. A.; Lin, L.; Car, R. Tunneling and delocalization effects in hydrogen bonded systems: A study in position and momentum space. *The Journal of Chemical Physics* **2008**, *130*, 204511
- (4) Pantalei, C.; Pietropaolo, A.; Senesi, R.; Imberti, S.; Andreani, C.; Mayers, J.; Burnham, C.; Reiter, G. Proton Momentum Distribution of Liquid Water from Room Temperature to the Supercritical Phase. *Physical Review Letters* **2008**, *100*, 177801
- (5) Burnham, C. J.; Anick, D. J.; Mankoo, P. K.; Reiter, G. F. The vibrational proton potential in bulk liquid water and ice. *The Journal of Chemical Physics* **2008**, *128*, 154519
- (6) Ramirez, R.; Herrero, C. P. Kinetic energy of protons in ice Ih and water: A path integral study. *Physical Review B* **2011**, *84*, 064130
- (7) Giuliani, A.; Bruni, F.; Ricci, M. A.; Adams, M. A. Isotope Quantum Effects on the Water Proton Mean Kinetic Energy. *Physical Review Letters* **2011**, *106*, 255502
- (8) Bruni, F.; Giuliani, A.; Mayers, J.; Ricci, M. A. Proton Momentum Distribution and Diffusion Coefficient in Water: Two Sides of the Same Coin? *The Journal of Physical Chemistry Letters* **2012**, *3*, 2594–2597, PMID: 26295880
- (9) Finkelstein, Y.; Moreh, R. Temperature dependence of the proton kinetic energy in water between 5 and 673 K. *Chemical Physics* **2014**, *431*, 58–63
- (10) Parmentier, A.; Shephard, J.J.; Romanelli G.; Senesi, R.; Salzmann, C.G.; Andreani, C. Evolution of Hydrogen Dynamics in Amorphous Ice with Density *The Journal of Physical Chemistry Letters* **2015**, *6*, 2038–2042
- (11) Andreani, C.; Colognesi, D.; Mayers, J.; Reiter, G. F.; Senesi, R. Measurement of momentum distribution of light atoms and molecules in condensed matter systems using inelastic neutron scattering. *Advances in Physics* **2005**, *54*, 377–469
- (12) Reiter, G. F.; Mayers, J.; Noreland, J. Momentum-distribution spectroscopy using deep inelastic neutron scattering. *Physical Review B* **2002**, *65*, 104305

- (13) Hohenberg, P. C.; Platzman, P. M. High-Energy Neutron Scattering from Liquid He⁴. *Physical Review* **1966**, *152*, 198–200
- (14) Gol'danskii, V. I. On Molecular Neutronoscopy. *Soviet Physics JETP* **1957**, *4*, 604
- (15) Ivanov, G. K.; Sayasov, Y. S. Theory of the Vibrational Excitation of a Molecule in the Impulse Approximation. *Soviet Physics Doklady* **1964**, *9*, 171
- (16) Reiter, G. F.; Senesi, R.; Mayers, J. Changes in the Zero-Point Energy of the Protons as the Source of the Binding Energy of Water to A-Phase DNA. *Physical Review Letters* **2010**, *105*, 148101
- (17) Krzystyniak, M.; Adams, M. A.; Lovell, A.; Skipper, N. T.; Bennington, S. M.; Mayers, J.; Fernandez-Alonso, F. Probing the binding and spatial arrangement of molecular hydrogen in porous hosts via neutron Compton scattering. *Faraday Discuss* **2011**, *151*, 171–197
- (18) Gunn, J. M. F.; Andreani, C.; Mayers, J. A new approach to impulsive neutron scattering. *Journal of Physics C Solid State Physics* **1986**, *19*, L835–L840
- (19) West, G. B. Electron scattering from atoms, nuclei and nucleons. *Physics Reports* **1975**, *18*, 263–323
- (20) Reiter, G.; Silver, R. Measurement of Interionic Potentials in Solids Using Deep-Inelastic Neutron Scattering. *Physical Review Letters* **1985**, *54*, 1047–1050
- (21) Watson, G. I. Neutron Compton scattering. *Journal of Physics Condensed Matter* **1996**, *8*, 5955–5975
- (22) Andreani, C.; Romanelli, G.; Senesi, R. A combined INS and DINS study of proton quantum dynamics of ice and water across the triple point and in the supercritical phase. *Chemical Physics* **2013**, *427*, 106–110
- (23) Romanelli, G.; Ceriotti, M.; Manolopoulos, D. E.; Pantalei, C.; Senesi, R.; Andreani, C. Direct Measurement of Competing Quantum Effects on the Kinetic Energy of Heavy Water upon Melting. *The Journal of Physical Chemistry Letters* **2013**, *4*, 3251–3256
- (24) Senesi, R.; Flammini, D.; Kolesnikov, A. I.; Éamonn D. Murray;; Galli, G.; Andreani, C. The quantum nature of the OH stretching mode in ice and water probed by neutron scattering experiments. *The Journal of Chemical Physics* **2013**, *139*, 074504
- (25) Flammini, D.; Pietropaolo, A.; Senesi, R.; Andreani, C.; McBride, F.; Hodgson, A.; Adams, M. A.; Lin, L.; Car, R. Spherical momentum distribution of the protons in hexagonal ice from modeling of inelastic neutron scattering data . *The Journal of Chemical Physics* **2012**, *136*, 024504
- (26) Pietropaolo, A.; Senesi, R.; Andreani, C.; Botti, A.; Ricci, M. A.; Bruni, F. Excess of Proton Mean Kinetic Energy in Supercooled Water. *Physical Review Letters* **2008**, *100*, 127802

- (27) Pietropaolo, A.; Senesi, R.; Andreani, C.; Mayers, J. Quantum Effects in Water: Proton Kinetic Energy Maxima in Stable and Supercooled Liquid. *Brazilian Journal of Physics* **2009**, 39, 318–321
- (28) Flammini, D.; Ricci, M. A.; Bruni, F. A new water anomaly: The temperature dependence of the proton mean kinetic energy. *The Journal of Chemical Physics* **2009**, 130, 236101
- (29) Cheng, B.; Behler, J.; Ceriotti, M. Private Communications
- (30) Senesi, R.; Andreani, C.; Bowden, Z.; Colognesi, D.; Degiorgi, E.; Fielding, A. L.; Mayers, J.; Nardone, M.; Norris, J.; Praitano, M. et al. VESUVIO: a novel instrument for performing spectroscopic studies in condensed matter with eV neutrons at the ISIS facility. *Physica B Condensed Matter* **2000**, 276, 200–201
- (31) Pietropaolo, A.; Senesi, R. Electron Volt neutron spectrometers. *Physics Reports* **2011**, 508, 45–90
- (32) Mayers, J.; Reiter, G. The VESUVIO electron volt neutron spectrometer. *Measurement Science and Technology* **2012**, 23, 045902
- (33) Seel, A.J.; Krzystyniak, M and Fernandez-Alonso, F. The VESUVIO Spectrometer Now and When? *Journal of Physics: Conference Series* **2014**, 571, 012006
- (34) Senesi, R.; Romanelli, G.; Adams, M. A.; Andreani, C. Temperature dependence of the zero point kinetic energy in ice and water above room temperature. *Chemical Physics* **2013**, 427, 111–116, PMID: 26266499
- (35) Perakis, F.; Hamm, P. Two-Dimensional Infrared Spectroscopy of Supercooled Water. *Journal of Phys. Chem.* **2011**, B 115, 5289
- (36) Ricci, M. A.; Nardone, M.; Fontana, A.; Andreani, C.; Hahn, W. Light and neutron scattering studies of the OH stretching band in liquid and supercritical water. *Journal of Chem. Phys.* **1998**, 108, 450